Title

Jet Definition and Transverse-Momentum—Dependent Factorization in Semi-inclusive Deep-Inelastic Scattering

Journal

Physical Review Letters, 134(6)

ISSN

0031-9007

Authors

Caucal, Paul
Iancu, Edmond
Mueller, AH
et al.

Publication Date

2025-02-14

DOI

10.1103/physrevlett.134.061903

Jet Definition and Transverse-Momentum–Dependent Factorization in Semi-inclusive Deep-Inelastic Scattering

Paul Caucal,[1,*] Edmond Iancu,[2,†] A. H. Mueller,[3,‡] and Feng Yuan[4,5,§]

[1]SUBATECH UMR 6457 (IMT Atlantique, Université de Nantes, IN2P3/CNRS), 4 rue Alfred Kastler, 44307 Nantes, France
[2]Université Paris-Saclay, CNRS, CEA, Institut de physique théorique, F-91191 Gif-sur-Yvette, France
[3]Department of Physics, Columbia University, New York, New York 10027, USA
[4]Nuclear Science Division, Lawrence Berkeley National Laboratory, Berkeley, California 94720, USA
[5]Institute for Theoretical Physics, Universität Tübingen, Auf der Morgenstelle 14, D-72076 Tübingen, Germany

(Received 6 September 2024; revised 18 November 2024; accepted 21 January 2025; published 12 February 2025)

Using the color dipole picture of deep inelastic scattering (DIS) and the color glass condensate effective theory, we study semi-inclusive jet production in DIS at small x in the limit where the photon virtuality Q^2 is much larger than the transverse momentum squared $P_\perp^2$ of the produced jet. In this limit, the cross section is dominated by aligned jet configurations, that is, quark–antiquark pairs in which one of the fermions—the would-be struck quark in the Breit frame—carries most of the longitudinal momentum of the virtual photon. We show that physically meaningful jet definitions in DIS are such that the effective axis of the jet sourced by the struck quark is controlled by its virtuality rather than by its transverse momentum. For such jet definitions, we show that the next-to-leading order cross section admits factorization in terms of the (sea) quark transverse momentum dependent distribution, which in turn satisfies a universal Dokshitzer-Gribov-Lipatov-Altarelli-Parisi and Sudakov evolution.

DOI: 10.1103/PhysRevLett.134.061903

Introduction—The semi-inclusive production of a hadron or a jet in deep-inelastic scattering (SIDIS) is a process of fundamental importance for the study of the partonic content inside a proton or a large nucleus. It allows for an unambiguous extraction of the quark and gluon distribution functions with increasing accuracy in perturbative QCD [1–6]. In the small transverse momentum region of the measured hadron or jet, it is sensitive to the transverse momentum dependent (TMD) quark distribution [7–10], whose precise extraction for both an unpolarized and polarized target is one of the main goals of the Electron-Ion Collider (EIC) physics program [11–13]. In this Letter, we consider the SIDIS process in the case of a jet measurement at small x_{Bj}, where the color glass condensate (CGC) effective theory [14–17] applies, and demonstrate that the factorization of the next-to-leading order (NLO) cross section in terms of the (sea) quark TMD necessitates the use a new jet reconstruction algorithm which captures the nontrivial dynamics of the quark struck by the virtual photon.

Compared to hadron production in SIDIS, jet production has the advantage that it can directly probe the TMD quark distribution without involving a TMD fragmentation function. However, a precise measurement of low transverse momentum jets is very challenging, in particular because the usual k_t-type algorithms may not be applicable. Alternative approaches and detailed phenomenology applications have been carried out in the last few years [18–35]. Together with these developments, the novel jet algorithm proposed in this paper will help to improve the precision of future jet measurements in SIDIS at the EIC and provide important probe to the nucleon-nucleus tomography in terms of the TMD quark distributions at various x ranges.

Aligned jet configurations—We work in the dipole frame (related to the Breit frame by a longitudinal boost) where the virtual photon has four momentum $q^\mu = [q^+, q^- = -Q^2/(2q^+), \mathbf{0}_\perp]$ and a nucleon from the nucleus target has four momentum $P_N^\mu = (0, P_N^-, \mathbf{0}_\perp)$ in light-cone coordinates. The standard DIS variables are defined by $Q^2 = -q^2$ and $x_{\mathrm{Bj}} = Q^2/\hat{s}$ with $\hat{s} = 2q^+P_N^-$. At LO in the color dipole picture of DIS at small x_{Bj} [36–39], the transversely polarized virtual photon γ_T^* splits into a quark–antiquark pair that interacts with the nucleus target. We denote by $k_{1,2}^\mu$ the four momenta of the quark and the antiquark and define $z_i = k_i^+/q^+$. Each outgoing parton can then form a jet for

*Contact author: caucal@subatech.in2p3.fr
†Contact author: edmond.iancu@ipht.fr
‡Contact author: ahm4@columbia.edu
§Contact author: fyuan@lbl.gov

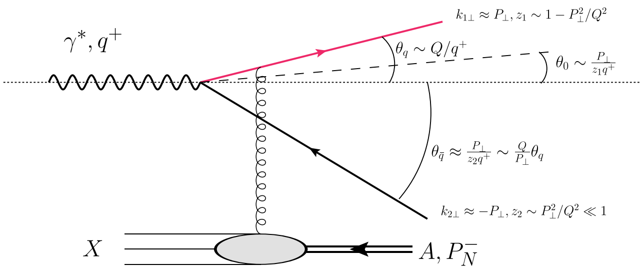

FIG. 1. Geometric representation of the typical aligned jet configuration at small x_{Bj} in the dipole frame.

which one only measures the transverse momentum $\boldsymbol{P}_\perp$. We are primarily interested in the limit $Q^2 \gg P_\perp^2$. The leading power in the $P_\perp^2/Q^2$ expansion of the cross section comes from aligned-jet configurations [40–42], that is very asymmetric $q\bar{q}$ pairs such that the quark has $1-z_1 \sim P_\perp^2/Q^2 \ll 1$ and carries most of the longitudinal momentum of the virtual photon while the antiquark has $z_2 \sim P_\perp^2/Q^2 \ll 1$, or vice versa (cf. Fig. 1). The struck fermion in the target picture is naturally the one with $z_i \sim 1$, yet the tagged jet with transverse momentum $\boldsymbol{P}_\perp$ can be either the fast ($z_i \sim 1$), or the slow ($z_i \ll 1$), fermion in the dipole picture. In the Breit frame, this would give either a forward jet in the direction of the photon, or a backward jet close to the beam remnants.

In the limit $Q^2 \gg P_\perp^2$, the semi-inclusive single jet cross section admits TMD factorization [41] in terms of the sea quark TMD $x\mathcal{F}_q(x, \boldsymbol{P}_\perp)$ at small x [40,43,44]:

$$\left.\frac{d\sigma^{\gamma_{\mathrm{T}}^*+A\to j+X}}{d^2\boldsymbol{P}_\perp}\right|_{\mathrm{LO}} = \frac{8\pi^2\alpha_{\mathrm{em}}e_f^2}{Q^2}x\mathcal{F}_q^{(0)}(x, \boldsymbol{P}_\perp), \tag{1}$$

where $x = x_{\mathrm{Bj}}$ as a consequence of minus momentum conservation. The superscript (0) for $\mathcal{F}_q$ refers to a LO approximation for the quark TMD including its high energy Balitsky-Kovchegov (BK) and Jalilian-Marian-Iancu-McLerran-Weigert-Leonidov-Kovner (JIMWLK) evolutions [45–53] down to the value of x of interest. α_{em} is the fine structure constant and e_f is the fractional electric charge of a light quark. This expression covers the case where the quark jet is measured [54], but it is inclusive in the jet longitudinal momentum fraction z. Explicit expression for the sea quark TMD in term of the quark–antiquark dipole S matrix at small x can be found in [41,56,57] (see also the Supplemental Material [58] for a brief review).

Heuristic discussion of the Sudakov logarithm—At NLO in the strong coupling α_s, the dominant radiative corrections to Eq. (1) are enhanced by double Sudakov logarithms [82–85] in the ratio of $Q^2/P_\perp^2$. To DLA, these Sudakov logarithms come from virtual emissions by the struck quark in the phase space that is forbidden to the real gluon emissions, that is real gluons which would modify the structure of the final state [86,87]. Clearly, the real gluon emissions with transverse momenta such that $k_{g\perp}^2 \gg P_\perp^2$ must be forbidden. On the other hand, virtual emissions with $k_{g\perp}^2 \geq Q^2$ do not have any double logarithmic support (the UV logarithmic divergence cancels above the hard scale Q^2 among virtual graphs [88]). The transverse phase-space which contributes to the Sudakov double logarithm is therefore $P_\perp^2 \ll k_{g\perp}^2 \ll Q^2$. Concerning the longitudinal phase space, we observe that the gluon emission must have a formation time $\tau_g = 1/k_g^-$ larger than the coherence time $\tau_\gamma = 1/|q^-|$ of the virtual photon [89–92]. In the context of high energy factorization, this condition is imposed on any gluon emission which does not contribute to the (collinearly improved) BK/JIMWLK evolution [45–53] of the target wave function. In terms of $z_g = k_g^+/q^+$, this gives the constraint $z_g \gg k_{g\perp}^2/Q^2$. We thus end up with the following integral for the Sudakov double logarithm,

$$S_{\mathrm{DL}} = -\frac{\alpha_s C_F}{2\pi}\int_{P_\perp^2}^{Q^2}\frac{dk_{g\perp}^2}{k_{g\perp}^2}\int_{k_{g\perp}^2/Q^2}^{z_{\max}}\frac{dz_g}{z_g}, \tag{2}$$

which factorizes from the LO cross section Eq. (1).

Consider now the upper limit $z_{\max}$ of the z_g integral. In the case of a *hadron* measurement, a forbidden real gluon must be well separated from the collinear singularity for a final-state emission. This singularity corresponds to (soft) gluons obeying $\boldsymbol{k}_{g\perp} = z_g\boldsymbol{P}_\perp/z_1$, with $z_1 \simeq 1$ for the struck quark. Clearly such collinear gluons have no overlap with the forbidden phase space at $k_{g\perp}^2 \gg P_\perp^2$, so the collinear singularity introduces no additional constraint on this phase space. We can then take $z_{\max} = 1$, which gives

$$S_{\mathrm{DL}}^{\mathrm{had}} = -\frac{\alpha_s C_F}{2\pi}\ln^2\left(\frac{Q^2}{P_\perp^2}\right), \tag{3}$$

as expected for hadron production [56,93].

The case of a *jet* measurement is considerably more subtle, and here comes our main physical observation. The fast quark with $z_1 \sim 1$ (see Fig. 1) is not put on-shell by the scattering, rather it emerges from the collision with a relatively large virtuality, of order Q^2. Indeed, after the photon decay $\gamma \to q\bar{q}$, the two quarks separate via quantum diffusion. By the time $\tau_\gamma = 2q^+/Q^2$ of the collision with the target, the wave packets of the fast quark and the slow antiquark spread out over distances $\Delta x_{q\perp}^2 \sim \tau_\gamma/(z_1 q^+)$ and $\Delta x_{\bar{q}\perp}^2 \sim \tau_\gamma/(z_2 q^+)$, respectively. In the aligned jet limit, $\Delta x_{q\perp}^2 \sim 1/Q^2$ and $\Delta x_{\bar{q}\perp}^2 \sim 1/P_\perp^2$. For the fast quark, $\Delta x_{q\perp}^2 \ll 1/P_\perp^2$ is very small, showing that this parton is still localized by its virtuality. Physically, this is so since the collision occurs relatively fast: $\tau_\gamma = 2q^+/Q^2$ is much smaller than the formation time $\tau_q \sim 2z_1 q^+/P_\perp^2$ for the fast quark. Accordingly, the angle made by this quark with respect to the collision axis by the time of scattering can be estimated as $\theta_q \sim \Delta x_{q\perp}/\tau_\gamma \sim Q/q^+$, which is much bigger than the naive angle $\theta_0 \sim P_\perp/q^+$ it would have made if it was on-shell (i.e., localized by its transverse momentum, see Fig. 1).

In order to be forbidden, a real gluon emission must not be part of the jet sourced by the fast quark. This condition imposes $\theta_g \sim k_{g\perp}/k_g^+ \gg \theta_q$, i.e., $z_g \ll k_{g\perp}/Q$. Using $z_{\max} = k_{g\perp}/Q$ in Eq. (2), one finds

$$S_{\mathrm{DL}}^{\mathrm{jet}} = -\frac{\alpha_s C_F}{4\pi} \ln^2\left(\frac{Q^2}{P_\perp^2}\right). \tag{4}$$

Thus, remarkably, the Sudakov corresponding to a jet final state is smaller by a factor of 2 than that for a hadron final state. This is so since the fast virtual quark generates a relatively wide jet, so the phase space that is forbidden to real emission is correspondingly smaller.

A new jet distance measure in DIS—To properly reflect the above physical picture, a jet measurement in DIS must be endowed with a clustering algorithm that accounts for the high virtuality $\sim Q^2$ of the struck quark. This is generally not the case for the jet algorithms that are *a priori* designed for hadron-hadron collisions, such as the k_t algorithms [94–98]: when applied to DIS, they typically cluster particles "around" an axis with angle $P_\perp/(zq^+)$ in the dipole frame [99–106] and thus do not capture the effect of the large virtuality of the jet with $z \sim 1$. Related to that, they fail to cluster the remnant of the struck quark into the same jet, as noted in [26]. In order to cope with these issues, we introduce a new jet distance measure, via

$$d_{ij} = \frac{M_{ij}^2}{(z_i z_j)^p Q^2 R^2}, \qquad d_{iB} = 1, \tag{5}$$

where d_{ij} is the distance between two particles labeled i, j, and d_{iB} is the particle-beam distance [107]. The measure depends on the invariant mass squared $M_{ij}^2 = (k_i + k_j)^2$ and the longitudinal momentum fractions $z_i = k_i \cdot P_N/(q \cdot P_N)$. For a given list of final state particles, the jet algorithm then runs inclusively [108] through pairwise recombination of particles i_0, j_0 if $d_{i_0 j_0}$ is minimal among all d_{ij}, d_{iB}, d_{jB}, while declaring i_0 a final state jet if $d_{i_0 B}$ is minimal, until no particle remains.

The algorithm depends on two parameters, the jet radius R and the power p. With $p = -1, 0, 1$, it gives, respectively, a k_t, mass, or angular ordered clustering in the dipole frame. We shall focus here on the specific choice $p = 1$, which is dynamically favored, as we shall shortly argue. With this choice, one finds (in the dipole frame and in the limit of a small relative angle $\theta_{ij} \ll 1$)

$$d_{ij} \approx \frac{\theta_{ij}^2 (q^+)^2}{Q^2 R^2}, \quad \text{for } p = 1. \tag{6}$$

Using this criterion at NLO, where the final state is made of two partons, the quark i and gluon j, one sees that these two partons are clustered within the same jet if $\theta_{ij} \leq R\theta_q$ with $\theta_q \sim Q/q^+$, in agreement with the dynamics of the fast virtual quark that we have just elucidated. This is a consequence of both the normalization of the distance measure with Q^2 and the choice of p. We assume the jet radius R to be small, but not *too* small, so that an additional $\ln(1/R)$ resummation is not needed [109,110].

For $p = 1$ and in the fragmentation region of the struck quark in the Breit frame, the algorithm is akin to generalized k_t algorithms originally designed for e^+e^- annihilation [98,112–114] and subsequently extended to DIS in [115,116] (cf. Supplemental Material [58]). However, unlike the latter, which are only defined in the Breit frame, Eq. (5) is longitudinally invariant by boost along the γ^*-A collision axis (see also [26,117]), so that d_{ij}, d_{iB} can be computed either in the Breit frame, or the dipole frame. This makes the distance measure Eq. (5) more convenient for higher order calculations and jet studies in DIS.

TMD factorization at NLO—For the *inclusive* production of jets in DIS, that is, in situations where the jet transverse momenta are not measured, but only their number, it was known since [115,116] that special jet definitions are needed to guarantee the validity of the standard collinear factorization for the jet cross section. In what follows, we would like to demonstrate a similar property for the semi-inclusive production of a jet with a given $P_\perp$. Specifically, we will show that the NLO corrections to the jet cross section (as computed in the dipole picture) are consistent with TMD factorization—in the sense that they correctly generate the expected Dokshitzer-Gribov-Lipatov-Altarelli-Parisi (DGLAP) [118–120] and Collins-Soper-Sterman (CSS) [9,85,121,122] evolutions of the quark TMD—if and only if the quark and the gluon jets are separated from each other by using the jet distance (5) with $p = 1$. To show that, we consider a relatively hard jet, with $Q^2 \gg P_\perp^2 \gg Q_s^2$. In this regime and to lowest order in $Q_s^2/P_\perp^2$, the transverse momentum of the measured jet is either given by the recoil from a hard gluon emission with $\boldsymbol{k}_{g\perp} \sim -\boldsymbol{P}_\perp$ (real contribution) or by the target itself (virtual contribution).

For the real contribution, our starting point is the quark–antiquark-gluon Fock component of the virtual photon wave function and, more precisely, its contribution to the $\gamma_{\mathrm{T}}^* + A \to qg$ cross section, as obtained after integrating out the antiquark [123]. The quark and the gluon are nearly back-to-back: their transverse momentum imbalance $\boldsymbol{\ell}_\perp = \boldsymbol{k}_{g\perp} + \boldsymbol{k}_{1\perp}$ is small compared to the relative momentum $\boldsymbol{P}_\perp = z_g \boldsymbol{k}_{1\perp} - z_1 \boldsymbol{k}_{g\perp}$: $\ell_\perp \ll P_\perp$ and $z_1 + z_g \simeq 1$. In the CGC calculation, this process is shown to factorize in terms of the quark TMD as [125,126]

$$\frac{\mathrm{d}\sigma^{\gamma_{\mathrm{T}}^{*}+A\to qg+X}}{\mathrm{d}^2\boldsymbol{P}_\perp \mathrm{d}^2\boldsymbol{\ell}_\perp \mathrm{d}z_1 \mathrm{d}z_g} = \alpha_{\mathrm{em}} e_f^2 \alpha_s C_F \delta(1-z_1-z_g) \times \frac{2z_1[(P_\perp^2+\bar{Q}^2)^2+z_g^2P_\perp^4+z_1^2\bar{Q}^4]}{P_\perp^2[P_\perp^2+\bar{Q}^2]^3} x_q \mathcal{F}_q^{(0)}(x_q,\boldsymbol{\ell}_\perp), \tag{7}$$

with $\bar{Q}^2 = z_1 z_g Q^2$ and $x_q = (M_{qg}^2 + Q^2)/\hat{s}$. The contribution of (7) to SIDIS is obtained by integrating out the kinematics of the unmeasured jet over the region in phase space where the quark and the gluon form two separated jets. Using the jet definition Eq. (5) with $p = 1$, the associated phase space constraint reads $P_\perp^2 \geq R^2 Q^2 z_1^2 z_g^2$. The subsequent integrals over z_1 and z_g are controlled by $z_1 \simeq 1$ and $z_g \lesssim P_\perp/(RQ) \ll 1$, so only relatively soft gluons contribute. Such soft gluons can be transferred into the target wave function [124,125,127,128] via a change of variable $z_g \to \xi$, with

$$z_g = \frac{\xi}{1-\xi}\frac{P_\perp^2}{Q^2} \Leftrightarrow \xi = \frac{x_{\mathrm{Bj}}}{x_q}, \tag{8}$$

where we have also used $M_{qg}^2 = P_\perp^2/(z_1 z_g)$ and $z_1 \simeq 1$. The integral over ξ is restricted to $x_{\mathrm{Bj}} < \xi < 1 - RP_\perp/Q$, where the upper limit is introduced by the jet constraint $z_g \lesssim P_\perp/(RQ)$, while the lower limit comes from the condition $x_q \leq 1$. Note that Eq. (7) is not singular as $z_g \to 0$ meaning that the contribution from Eq. (7) to the NLO cross section does not overlap with the high energy evolution already accounted for through the x dependence of $x\mathcal{F}_q^{(0)}$ in Eq. (1). Finally, the integral over the momentum imbalance $\ell_\perp \ll P_\perp$ builds the quark PDF xf_q on the resolution scale of the hard jet:

$$xf_q^{(0)}(x, P_\perp^2) = \int_{\Lambda^2}^{P_\perp^2} \mathrm{d}^2\boldsymbol{\ell}_\perp x\mathcal{F}_q^{(0)}(x,\boldsymbol{\ell}_\perp), \tag{9}$$

with Λ of the order of the QCD confinement scale. Based on the above, a straightforward calculation yields

$$\left.\frac{\mathrm{d}\sigma^{\gamma_{\mathrm{T}}^{*}+A\to j+X}}{\mathrm{d}^2\boldsymbol{P}_\perp}\right|_R = \frac{8\pi^2\alpha_{\mathrm{em}}e_f^2}{Q^2}\frac{\alpha_s}{2\pi^2}\frac{1}{P_\perp^2}\int_{x_{\mathrm{Bj}}}^{1-\frac{RP_\perp}{Q}} \mathrm{d}\xi \times P_{qq}(\xi)\frac{x_{\mathrm{Bj}}}{\xi} f_q^{(0)}\left(\frac{x_{\mathrm{Bj}}}{\xi}, P_\perp^2\right), \tag{10}$$

with $P_{qq}(\xi) = C_F(1+\xi^2)/(1-\xi)$ the unregularized $q \to qg$ splitting function. In Eq. (10) we included a factor of 2 to account for the fact that the tagged jet can be generated by either the fast quark ($z_1 \simeq 1$), or the slow gluon ($z_g \ll 1$). The NLO correction in Eq. (10) exhibits TMD factorization, as anticipated: the expression in the second line can be interpreted as an evolution of the quark TMD. The singularity of $P_{qq}(\xi)$ at $\xi = 1$ introduces a logarithmic sensitivity to the upper limit, that can be isolated with the help of the plus prescription:

$$x\mathcal{F}_q^{(1)}(x, P_\perp, Q^2)|_{\boldsymbol{R}} = \frac{\alpha_s}{2\pi^2}\frac{1}{P_\perp^2}\int_x^1 \mathrm{d}\xi P_{qq}^{(+)}(\xi)\frac{x}{\xi}f_q^{(0)}\left(\frac{x}{\xi}, P_\perp^2\right) + \frac{\alpha_s C_F}{2\pi^2}\frac{1}{P_\perp^2}\ln\left(\frac{Q^2}{R^2P_\perp^2}\right)xf_q^{(0)}(x, P_\perp^2), \tag{11}$$

where $P_{qq}^{(+)}(\xi)$ differs from $P_{qq}(\xi)$ only via the replacement $(1-\xi) \to (1-\xi)_+$ in the denominator. We recognize in Eq. (11) one (real) step in the DGLAP + CSS evolution of the quark TMD. (See also [124,125] for similar arguments.) As shown in the Supplemental Material [58], Eq. (11) is also the standard result for the one-loop contribution of the collinear gluon radiation to the quark TMD at moderate x and $P_\perp \gg \Lambda$ [10]. Recovering this well-known result is a nontrivial check of our jet definition. Indeed, the precise coefficient of the Sudakov logarithm in the second line is a consequence of choosing $p = 1$ in our jet distance measure (5). If one were using another jet definition from that class, or a definition with an effective jet axis set by the angle θ_0 in Fig. 1, the upper limit of the ξ integral in Eq. (10) would change (e.g., it would be $\xi < 1 - R^2P_\perp^2/Q^2$ for $p = 0$), which would in turn modify the normalization of the Sudakov logarithm. With $p = -1$ in Eq. (5), the quark and the gluon would typically be clustered within the same jet, so that the TMD evolution that we have just unveiled would not be resolved within the wide jet formed by the struck quark.

An important consistency check refers to the detailed balance between the real and the virtual NLO corrections: after integrating the cross-section over $\boldsymbol{P}_\perp$, the Sudakov logarithms must cancel between real and virtual terms (see, e.g., the discussion in [124]). In order to verify this condition and also to complete our calculation of the cross section to the accuracy of interest, we need the virtual NLO contributions in the limit $Q^2 \gg P_\perp^2 \gg Q_s^2$. They can be inferred from the NLO calculation of the SIDIS cross section in the CGC, as presented in [88]. The details of the leading power extraction in these expressions are provided in Supplemental Material [58]. The virtual terms too are sensitive to the jet definition, as clear from the fact that they include the phase-space region where the quark and the gluon are nearly collinear with each other and hence must be clustered within the same jet. The collinear singularity cancels between real and virtual contributions, but the finite reminder, which is enhanced by (double and single) Sudakov logarithms, is clearly dependent upon our definition for the jets. Using Eq. (5) with $p = 1$, the virtual term reads.

$$\left.\frac{\mathrm{d}\sigma^{\gamma_T^*+A\to j+X}}{\mathrm{d}^2\boldsymbol{P}_\perp}\right|_V = \left.\frac{\mathrm{d}\sigma^{\gamma_T^*+A\to j+X}}{\mathrm{d}^2\boldsymbol{P}_\perp}\right|_{\mathrm{LO}} \times \frac{\alpha_s C_F}{\pi}\left[-\frac{1}{4}\ln^2\left(\frac{Q^2}{P_\perp^2}\right) + \left(\frac{3}{4}+\ln(R)\right)\ln\left(\frac{Q^2}{P_\perp^2}\right) - \frac{3}{2}\ln(R) + \frac{11}{4} - \frac{3\pi^2}{4} + \frac{3}{4}\ln^2(x_\star) + \frac{3}{8}\ln(x_\star) + \mathcal{O}(R^2)\right]. \tag{12}$$

where $x_\star$ is a $\mathcal{O}(1)$ number that marks the separation between the phase spaces $z_g \leq x_\star k_{g\perp}^2/Q^2$ contributing to collinearly improved BK/JIMWLK evolution [89–92] of the quark TMD, and $z_g \geq x_\star k_{g\perp}^2/Q^2$ contributing to the NLO impact factor. Since the latter has undergone a power expansion in $P_\perp/Q$ and $Q_s/P_\perp$, unlike the former, the cancellation of the $x_\star$ dependence between small x evolution and NLO impact factor is not complete anymore, but the remaining $x_\star$ dependence is a pure NLO effect, as clear from Eq. (12).

The first term in the square bracket in Eq. (12) is the Sudakov double logarithm that we heuristically derived in Eq. (4). It agrees with the expectation from the CSS kernel for the quark TMD alone [9,85,121,122]. The second term is a Sudakov single logarithm, which depends both on the quark anomalous dimension $\Gamma_q = (3\alpha_s C_F/4\pi)$ and on the jet parameter R. By only keeping these logarithmic terms, one obtains the virtual contribution to the DGLAP + CSS evolution of the quark TMD:

$$\begin{aligned} &x\mathcal{F}_q^{(1)}(x,\boldsymbol{P}_\perp,Q^2)|_V \\ &= -\frac{\alpha_s C_F}{2\pi} x\mathcal{F}_q^{(0)}(x,\boldsymbol{P}_\perp) \\ &\quad\times\left[\frac{1}{2}\ln^2\left(\frac{Q^2}{P_\perp^2}\right) - \left(\frac{3}{2}+\ln(R^2)\right)\ln\left(\frac{Q^2}{P_\perp^2}\right)\right]. \end{aligned} \tag{13}$$

After integrating Eqs. (11) and (13) over $P_\perp^2$ up to Q^2, it is straightforward to verify that the effects of the Sudakov logarithms which are manifest in these two equations mutually cancel, as announced. Furthermore, the piece 3/2 in Eq. (13) gives a contribution $(3/2)\delta(1-\xi)$ to the splitting function in Eq. (11), thus completing the standard expression for the regularized DGLAP splitting function $\mathcal{P}_{qq}(\xi)$ [9]. This real vs virtual cancellation is a crucial feature of the jet definition that we employed, i.e., Eq. (5) with $p = 1$ (we show in Supplemental Material [58] that other common choices of DIS jet definitions do not satisfy this condition). We thus obtain the DGLAP equation for the quark PDF in integral form:

$$\begin{aligned} xf_q(x,Q^2) = xf_q^{(0)}(x,Q^2) + \int_{\Lambda^2}^{Q^2}\frac{\mathrm{d}P_\perp^2}{P_\perp^2}\frac{\alpha_s(P_\perp^2)}{2\pi} \\ \times\int_x^1 \mathrm{d}\xi\mathcal{P}_{qq}(\xi)\frac{x}{\xi}f_q\left(\frac{x}{\xi},P_\perp^2\right), \end{aligned} \tag{14}$$

where we have also inserted a running coupling, as standard in this context. The CSS equation obeyed by the quark TMD can be obtained by taking a derivative w.r.t. $\ln Q^2$ in the sum of Eqs. (11) and (13). The precise relation between our "top-down" approach [124] to the resummation of Sudakov logarithms and the standard CSS formalism is given by $x\mathcal{F}_q(x,\boldsymbol{P}_\perp,Q^2) = x\mathcal{F}_q^{(\mathrm{sub})}(x,\boldsymbol{P}_\perp,\mu_F = Q,\zeta_c = Q)$, where $\mathcal{F}_q^{(\mathrm{sub})}$ is the subtracted quark TMD in the Collins-11 scheme [9] and μ_F, ζ_c are, respectively, the UV and rapidity renormalization scales, both identified with the hard scale Q of the process [129]. As shown in [130,131], this diagonal scheme also has the advantage of preserving the validity of Eq. (9) connecting the quark TMD to the quark PDF [with $x\mathcal{F}_q^{(0)} \to x\mathcal{F}_q(x,\boldsymbol{\ell}_\perp,P_\perp^2)$] up to $\mathcal{O}(\alpha_s^2)$ corrections.

In the end, the single inclusive jet cross section at small x and $Q^2 \gg P_\perp^2 \gg Q_s^2$, for our new jet distance measure can be written

$$\begin{aligned} \left.\frac{\mathrm{d}\sigma^{\gamma_T^*+A\to j+X}}{\mathrm{d}^2\boldsymbol{P}_\perp}\right|_{\mathrm{NLO}} &= \frac{8\pi^2\alpha_{\mathrm{em}}e_f^2}{Q^2}x\mathcal{F}_q(x,\boldsymbol{P}_\perp,Q^2) \\ &\quad\times\left[1-\frac{3\alpha_s C_F}{2\pi}\ln(R)+\mathcal{O}(\alpha_s)\right], \end{aligned} \tag{15}$$

where all the potentially large logarithms $\alpha_s\ln(1/x)$, $\alpha_s\ln(P_\perp^2/\Lambda^2)$, $\alpha_s\ln^2(Q^2/P_\perp^2)$ and $\alpha_s\ln(Q^2/P_\perp^2)$ are resummed within the quark TMD via BK/JIMWLK—or Balitsky-Fadin-Kuraev-Lipatov (BFKL) [132,133] in the dilute limit $P_\perp \gg Q_s$—and DGLAP + CSS evolution equations, respectively.

To summarize, we have demonstrated that TMD factorization for jet production in SIDIS is not guaranteed by all jet definitions and we have designed a longitudinally invariant jet clustering algorithm which preserves both the factorization and the universality of the DGLAP + CSS evolution of the quark TMD at small x. Physically, this jet definition is able to resolve the DGLAP and Sudakov dynamics of the struck sea quark and to distinguish the backward antiquark jet (in the Breit frame) from the beam remnant. While these results are derived in the context of the high energy factorization, they also apply at moderate values of x, as demonstrated in the Supplemental Material [58], where we find a similar factorization property by following the dynamics of the struck quark in the target picture. Once again, the proper choice of the jet definition turns out to be essential to ensure the correct matching between the NLO corrections to

SIDIS and the DGLAP + CSS evolution of the quark TMD. It will be important to investigate further the jet definition Eq. (5) both at small and moderate x, as we anticipate that it could be of great importance for the forthcoming quark tomography at the EIC with jets [24,25].

Acknowledgments—We are grateful to Cyrille Marquet, Farid Salazar, Gregory Soyez, and Werner Vogelsang for inspiring discussions. We thank the France-Berkeley-Fund from University of California at Berkeley for support. The work of F. Y. is supported in part by the U.S. Department of Energy, Office of Science, Office of Nuclear Physics, under Contract No. DE-AC02-05CH11231. The work of A. H. M. is supported in part by the U.S. Department of Energy Grant No. DE-FG02-92ER40699.

[1] G. Altarelli, R. K. Ellis, G. Martinelli, and S.-Y. Pi, Nucl. Phys. **B160**, 301 (1979).
[2] R. Baier and K. Fey, Z. Phys. C **2**, 339 (1979).
[3] D. de Florian, M. Stratmann, and W. Vogelsang, Phys. Rev. D **57**, 5811 (1998).
[4] G. Abelof, R. Boughezal, X. Liu, and F. Petriello, Phys. Lett. B **763**, 52 (2016).
[5] S. Goyal, S.-O. Moch, V. Pathak, N. Rana, and V. Ravindran, Phys. Rev. Lett. **132**, 251902 (2024).
[6] L. Bonino, T. Gehrmann, and G. Stagnitto, Phys. Rev. Lett. **132**, 251901 (2024).
[7] J. C. Collins, Nucl. Phys. **B396**, 161 (1993).
[8] X.-d. Ji, J.-p. Ma, and F. Yuan, Phys. Rev. D **71**, 034005 (2005).
[9] J. Collins, *Foundations of Perturbative QCD*, Cambridge Monographs on Particle Physics, Nuclear Physics and Cosmology (Cambridge University Press, Cambridge, England, 2023), Vol. 32.
[10] R. Boussarie *et al.*, arXiv:2304.03302.
[11] A. Accardi *et al.*, Eur. Phys. J. A **52**, 268 (2016).
[12] R. Abdul Khalek *et al.*, Nucl. Phys. **A1026**, 122447 (2022).
[13] P. Achenbach *et al.*, Nucl. Phys. **A1047**, 122874 (2024).
[14] E. Iancu, A. Leonidov, and L. McLerran, in *Cargese Summer School on QCD Perspectives on Hot and Dense Matter* (2002), pp. 73–145, arXiv:hep-ph/0202270.
[15] E. Iancu and R. Venugopalan, The Color glass condensate and high-energy scattering in QCD, in *Quark-Gluon Plasma 4*, edited by R. C. Hwa and X.-N. Wang (2003), pp. 249–3363, arXiv:hep-ph/0303204.
[16] F. Gelis, E. Iancu, J. Jalilian-Marian, and R. Venugopalan, Annu. Rev. Nucl. Part. Sci. **60**, 463 (2010).
[17] Y. V. Kovchegov and E. Levin, *Quantum Chromodynamics at High Energy* (Oxford University Press, New York, 2013), Vol. 33.
[18] D. Gutierrez-Reyes, I. Scimemi, W. J. Waalewijn, and L. Zoppi, Phys. Rev. Lett. **121**, 162001 (2018).
[19] D. Gutierrez-Reyes, Y. Makris, V. Vaidya, I. Scimemi, and L. Zoppi, J. High Energy Phys. 08 (2019) 161.
[20] D. Gutierrez-Reyes, I. Scimemi, W. J. Waalewijn, and L. Zoppi, J. High Energy Phys. 10 (2019) 031.
[21] X. Liu, F. Ringer, W. Vogelsang, and F. Yuan, Phys. Rev. Lett. **122**, 192003 (2019).
[22] X. Liu, F. Ringer, W. Vogelsang, and F. Yuan, Phys. Rev. D **102**, 094022 (2020).
[23] E.-C. Aschenauer, K. Lee, B. S. Page, and F. Ringer, Phys. Rev. D **101**, 054028 (2020).
[24] B. S. Page, X. Chu, and E. C. Aschenauer, Phys. Rev. D **101**, 072003 (2020).
[25] M. Arratia, Y. Song, F. Ringer, and B. V. Jacak, Phys. Rev. C **101**, 065204 (2020).
[26] M. Arratia, Y. Makris, D. Neill, F. Ringer, and N. Sato, Phys. Rev. D **104**, 034005 (2021).
[27] M. Arratia, Z.-B. Kang, A. Prokudin, and F. Ringer, Phys. Rev. D **102**, 074015 (2020).
[28] Z.-B. Kang, X. Liu, S. Mantry, M. C. Spraker, and T. Wilson, Phys. Rev. D **103**, 074028 (2021).
[29] Z.-B. Kang, X. Liu, S. Mantry, and D. Y. Shao, Phys. Rev. Lett. **125**, 242003 (2020).
[30] Z.-B. Kang, K. Lee, D. Y. Shao, and F. Zhao, J. High Energy Phys. 11 (2021) 005.
[31] V. Andreev *et al.* (H1 Collaboration), Phys. Rev. Lett. **128**, 132002 (2022).
[32] W. K. Lai, X. Liu, M. Wang, and H. Xing, arXiv:2205.04570.
[33] K. Lee, J. Mulligan, M. Płoskoń, F. Ringer, and F. Yuan, J. High Energy Phys. 03 (2023) 085.
[34] M. Arratia, Z.-B. Kang, S. J. Paul, A. Prokudin, F. Ringer, and F. Zhao, Phys. Rev. D **107**, 094036 (2023).
[35] S. Fang, W. Ke, D. Y. Shao, and J. Terry, J. High Energy Phys. 05 (2024) 066.
[36] B. Z. Kopeliovich, L. I. Lapidus, and A. B. Zamolodchikov, JETP Lett. **33**, 595 (1981).
[37] G. Bertsch, S. J. Brodsky, A. S. Goldhaber, and J. F. Gunion, Phys. Rev. Lett. **47**, 297 (1981).
[38] A. H. Mueller, Nucl. Phys. **B335**, 115 (1990).
[39] N. N. Nikolaev and B. Zakharov, Z. Phys. C **49**, 607 (1991).
[40] A. H. Mueller, Nucl. Phys. **B558**, 285 (1999).
[41] C. Marquet, B.-W. Xiao, and F. Yuan, Phys. Lett. B **682**, 207 (2009).
[42] E. Iancu, A. H. Mueller, D. N. Triantafyllopoulos, and S. Y. Wei, J. High Energy Phys. 07 (2021) 196.
[43] L. D. McLerran and R. Venugopalan, Phys. Rev. D **59**, 094002 (1999).
[44] R. Venugopalan, Acta Phys. Pol. B **30**, 3731 (1999).
[45] I. Balitsky, Nucl. Phys. **B463**, 99 (1996).
[46] Y. V. Kovchegov, Phys. Rev. D **60**, 034008 (1999).
[47] J. Jalilian-Marian, A. Kovner, A. Leonidov, and H. Weigert, Nucl. Phys. **B504**, 415 (1997).
[48] J. Jalilian-Marian, A. Kovner, A. Leonidov, and H. Weigert, Phys. Rev. D **59**, 014014 (1998).
[49] A. Kovner, J. G. Milhano, and H. Weigert, Phys. Rev. D **62**, 114005 (2000).
[50] H. Weigert, Nucl. Phys. **A703**, 823 (2002).
[51] E. Iancu, A. Leonidov, and L. D. McLerran, Nucl. Phys. **B692**, 583 (2001).
[52] E. Iancu, A. Leonidov, and L. D. McLerran, Phys. Lett. B **510**, 133 (2001).
[53] E. Ferreiro, E. Iancu, A. Leonidov, and L. McLerran, Nucl. Phys. **A703**, 489 (2002).

[54] A similar expression holds for the case where the antiquark jet is measured. See [55] for a discussion of the unitarity of the SIDIS cross-section with jets.
[55] M. Cacciari, S. Forte, D. Napoletano, G. Soyez, and G. Stagnitto, Phys. Rev. D **100**, 114015 (2019).
[56] B.-W. Xiao, F. Yuan, and J. Zhou, Nucl. Phys. **B921**, 104 (2017).
[57] X.-B. Tong, B.-W. Xiao, and Y.-Y. Zhang, Phys. Rev. Lett. **130**, 151902 (2023).
[58] See Supplemental Material at http://link.aps.org/supplemental/10.1103/PhysRevLett.134.061903, which includes Refs. [59–81], for a comparison of the various jet definitions used in DIS, details on the derivation of Eq. (12) and a general discussion on TMD factorization for jet production in SIDIS at moderate values for *x*.
[59] P. R. Newman and M. Wing, Rev. Mod. Phys. **86**, 1037 (2014).
[60] S. Chekanov *et al.* (ZEUS Collaboration), Phys. Lett. B **547**, 164 (2002).
[61] S. Chekanov *et al.* (ZEUS Collaboration), Nucl. Phys. **A765**, 1 (2007).
[62] H. Abramowicz *et al.* (ZEUS Collaboration), Eur. Phys. J. C **70**, 965 (2010).
[63] A. Aktas *et al.* (H1 Collaboration), Phys. Lett. B **653**, 134 (2007).
[64] V. Andreev *et al.* (H1 Collaboration), Eur. Phys. J. C **77**, 215 (2017); **81**, 739(E) (2021).
[65] I. Abt *et al.* (ZEUS Collaboration), Eur. Phys. J. C **83**, 1082 (2023).
[66] X. Liu and F. Petriello, Phys. Rev. D **87**, 094027 (2013).
[67] S. Catani, Y. L. Dokshitzer, M. H. Seymour, and B. R. Webber, Nucl. Phys. **B406**, 187 (1993).
[68] G. C. Blazey *et al.*, in *Physics at Run II: QCD and Weak Boson Physics Workshop: Final General Meeting* (2000), pp. 47–77, arXiv:hep-ex/0005012.
[69] B. Ducloué, E. Iancu, G. Soyez, and D. Triantafyllopoulos, Phys. Lett. B **803**, 135305 (2020).
[70] F. Dominguez, C. Marquet, B.-W. Xiao, and F. Yuan, Phys. Rev. D **83**, 105005 (2011).
[71] F. Bergabo and J. Jalilian-Marian, Phys. Rev. D **106**, 054035 (2022).
[72] E. Iancu and Y. Mulian, J. High Energy Phys. 07 (2023) 121.
[73] F. Bergabo and J. Jalilian-Marian, Phys. Rev. D **107**, 054036 (2023).
[74] F. Bergabo and J. Jalilian-Marian, J. High Energy Phys. 01 (2023) 095.
[75] T. Becher and M. Neubert, Eur. Phys. J. C **71**, 1665 (2011).
[76] T. Becher, M. Neubert, and D. Wilhelm, J. High Energy Phys. 05 (2013) 110.
[77] M. G. Echevarria, A. Idilbi, and I. Scimemi, J. High Energy Phys. 07 (2012) 002.
[78] M. G. Echevarria, A. Idilbi, and I. Scimemi, Phys. Rev. D **90**, 014003 (2014).
[79] J.-Y. Chiu, A. Jain, D. Neill, and I. Z. Rothstein, J. High Energy Phys. 05 (2012) 084.
[80] M. A. Ebert, I. W. Stewart, and Y. Zhao, J. High Energy Phys. 03 (2020) 099.
[81] P. Sun and F. Yuan, Phys. Rev. D **88**, 114012 (2013).
[82] V. V. Sudakov, Sov. Phys. JETP **3**, 65 (1956).
[83] Y. L. Dokshitzer, D. Diakonov, and S. I. Troian, Phys. Rep. **58**, 269 (1980).
[84] G. Parisi and R. Petronzio, Nucl. Phys. **B154**, 427 (1979).
[85] J. C. Collins, D. E. Soper, and G. F. Sterman, Nucl. Phys. **B250**, 199 (1985).
[86] A. H. Mueller, B.-W. Xiao, and F. Yuan, Phys. Rev. Lett. **110**, 082301 (2013).
[87] A. Mueller, B.-W. Xiao, and F. Yuan, Phys. Rev. D **88**, 114010 (2013).
[88] P. Caucal, E. Ferrand, and F. Salazar, J. High Energy Phys. 05 (2024) 110.
[89] G. Beuf, Phys. Rev. D **89**, 074039 (2014).
[90] E. Iancu, J. Madrigal, A. Mueller, G. Soyez, and D. Triantafyllopoulos, Phys. Lett. B **744**, 293 (2015).
[91] Y. Hatta and E. Iancu, J. High Energy Phys. 08 (2016) 083.
[92] B. Ducloué, E. Iancu, A. H. Mueller, G. Soyez, and D. N. Triantafyllopoulos, J. High Energy Phys. 04 (2019) 081.
[93] T. Altinoluk, J. Jalilian-Marian, and C. Marquet, Phys. Rev. D **110**, 094056 (2024).
[94] S. D. Ellis and D. E. Soper, Phys. Rev. D **48**, 3160 (1993).
[95] Y. L. Dokshitzer, G. D. Leder, S. Moretti, and B. R. Webber, J. High Energy Phys. 08 (1997) 001.
[96] M. Wobisch and T. Wengler, in *Proceedings of the Workshop on Monte Carlo Generators for HERA Physics (Plenary Starting Meeting)* (1998), pp. 270–279, arXiv:hep-ph/9907280.
[97] M. Cacciari, G. P. Salam, and G. Soyez, J. High Energy Phys. 04 (2008) 063.
[98] M. Cacciari, G. P. Salam, and G. Soyez, Eur. Phys. J. C **72**, 1896 (2012).
[99] D. Y. Ivanov and A. Papa, J. High Energy Phys. 05 (2012) 086.
[100] R. Boussarie, A. Grabovsky, L. Szymanowski, and S. Wallon, J. High Energy Phys. 11 (2016) 149.
[101] K. Roy and R. Venugopalan, Phys. Rev. D **101**, 071505(R) (2020).
[102] K. Roy and R. Venugopalan, Phys. Rev. D **101**, 034028 (2020).
[103] P. Caucal, F. Salazar, and R. Venugopalan, J. High Energy Phys. 11 (2021) 222.
[104] P. Taels, T. Altinoluk, G. Beuf, and C. Marquet, J. High Energy Phys. 10 (2022) 184.
[105] P. Caucal, F. Salazar, B. Schenke, and R. Venugopalan, J. High Energy Phys. 11 (2022) 169.
[106] H.-y. Liu, K. Xie, Z. Kang, and X. Liu, J. High Energy Phys. 07 (2022) 041.
[107] The measure corresponds to the particular case $k = 0$ of a generalized distance measure $d_{ij} = \min(k_{i\perp}^{2k}, k_{j\perp}^{2k}) M_{ij}^2 / [(z_i z_j)^p Q^2 R^2]$, $d_{iB} = k_{i\perp}^{2k}$ as done in hadron-hadron collisions [97,108].
[108] G. P. Salam, Eur. Phys. J. C **67**, 637 (2010).
[109] M. Dasgupta, F. Dreyer, G. P. Salam, and G. Soyez, J. High Energy Phys. 04 (2015) 039.
[110] For jet production with a very small R, one needs to introduce the so-called semi-inclusive jet function [111]

and the factorization will be different from what we discuss in this Letter.

[111] Z.-B. Kang, F. Ringer, and I. Vitev, J. High Energy Phys. 10 (2016) 125.

[112] W. Bartel *et al.* (JADE Collaboration), Z. Phys. C **33**, 23 (1986).

[113] S. Bethke *et al.* (JADE Collaboration), Phys. Lett. B **213**, 235 (1988).

[114] S. Catani, Y. L. Dokshitzer, M. Olsson, G. Turnock, and B. R. Webber, Phys. Lett. B **269**, 432 (1991).

[115] S. Catani, Y. L. Dokshitzer, and B. R. Webber, Phys. Lett. B **285**, 291 (1992).

[116] B. R. Webber, J. Phys. G **19**, 1567 (1993).

[117] M. van Beekveld and S. Ferrario Ravasio, J. High Energy Phys. 02 (2024) 001.

[118] V. Gribov and L. Lipatov, Sov. J. Nucl. Phys. **15**, 438 (1972).

[119] G. Altarelli and G. Parisi, Nucl. Phys. **B126**, 298 (1977).

[120] Y. L. Dokshitzer, Sov. Phys. JETP **46**, 641 (1977).

[121] J. C. Collins and D. E. Soper, Nucl. Phys. **B193**, 381 (1981); **B213**, 545(E) (1983).

[122] J. C. Collins and D. E. Soper, Nucl. Phys. **B194**, 445 (1982).

[123] If instead of the antiquark, one integrates out the gluon, that is, if one computes a real-gluon correction to the $\gamma_T^* + A \to qq$ cross section, then one generates a step in the DGLAP + CSS evolution of the *gluon* TMD [124].

[124] P. Caucal and E. Iancu, arXiv:2406.04238.

[125] S. Hauksson, E. Iancu, A. H. Mueller, D. N. Triantafyllopoulos, and S. Y. Wei, J. High Energy Phys. 06 (2024) 180.

[126] P. Caucal, E. Iancu, F. Salazar, and F. Yuan (to be published).

[127] E. Iancu, A. H. Mueller, and D. N. Triantafyllopoulos, Phys. Rev. Lett. **128**, 202001 (2022).

[128] E. Iancu, A. H. Mueller, D. N. Triantafyllopoulos, and S. Y. Wei, J. High Energy Phys. 10 (2022) 103.

[129] For $\zeta_c = Q$, our longitudinal upper cutoff in $\xi \leq 1 - P_\perp/Q$ introduced the jet constraint is equivalent to the rapidity cutoff y_n in Collins-11 scheme defined as $\zeta_c^2 = 2(x_{\mathrm{Bj}} P_N^-) e^{2y_n}$.

[130] M. A. Ebert, J. K. L. Michel, I. W. Stewart, and Z. Sun, J. High Energy Phys. 07 (2022) 129.

[131] O. del Rio, A. Prokudin, I. Scimemi, and A. Vladimirov, Phys. Rev. D **110**, 016003 (2024).

[132] E. Kuraev, L. Lipatov, and V. S. Fadin, Sov. Phys. JETP **45**, 199 (1977).

[133] I. Balitsky and L. Lipatov, Sov. J. Nucl. Phys. **28**, 822 (1978).